Advanced Journal of Chemistry, Section A

Journal homepage: www.ajchem-a.com

Original Research Article

Synthesis and Characterization of Nano-Palm Oil Fuel Ash and Nano-Fly Ash as Cementitious Fillers in High-Performance Engineering Cementitious Composites

Shinta Marito Siregar[1,*], Fatimah Insani Harahap[2], Ridwanto Ridwanto[3], Khairiah Khairiah[1]

[1]*Faculty of Teacher Training and Education, Universitas Muslim Nusantara Al Washliyah, Jalan Garu II No. 93, Medan, Indonesia*
[2]*Faculty of Engineering, Universitas Sumatera Utara, Jalan Almamater Kampus USU, Medan, Indonesia*
[3]*Faculty of Pharmacy, Universitas Muslim Nusantara Al Washliyah, Jalan Garu II No. 93, Medan, Indonesia*

ARTICLEINFO

Article history

Submitted: 2025-10-22
Revised: 2025-11-06
Accepted: 2025-12-27
ID: AJCA-2510-1955
DOI: 10.48309/AJCA.2026.554924.1955

KEYWORDS

Palm oil fuel ash
Fly ash
Nanomortar
Engineered cementitious composites
Pozzolanic reactivity
Environmental sustainability

ABSTRACT

This study aims to enhance the pozzolanic reactivity and cementitious performance of palm oil fuel ash (POFA) and fly ash (FA) nanoparticles as eco-friendly supplementary materials in nanostructured engineered cementitious composites (ECC), thereby reducing industrial boiler waste and contributing to sustainable construction practices. POFA and FA were dried and ground into nanoparticles using a ball mill with replacement levels of 0%, 5%, 10%, and 15%. Characterization was performed using XRF, XRD, and FTIR, while physical tests included slump flow, density, and compressive strength. XRF confirmed the cementitious and pozzolanic properties of POFA and FA, with POFA containing over 50% SiO_2+Al_2O_3+Fe_2O_3 and FA exceeding 70%. XRD showed average crystal sizes of 28.02 nm (POFA) and 16.46 nm (FA) with amorphous phases of 71.78% and 91.93%, respectively. FTIR revealed dominant Si–O–Si and Si–OH groups, indicating high silica content and pozzolanic reactivity. The slump flow decreased with higher POFA and FA content due to water absorption but remained within the high-performance concrete range (500–800 mm). Density values decreased yet stayed between normal and lightweight concrete limits. The compressive strength increased with higher nanoparticle content, reaching 46.34–72.73 MPa at 28 days, confirming improved hydration and mechanical performance.

GRAPHICALABSTRACT

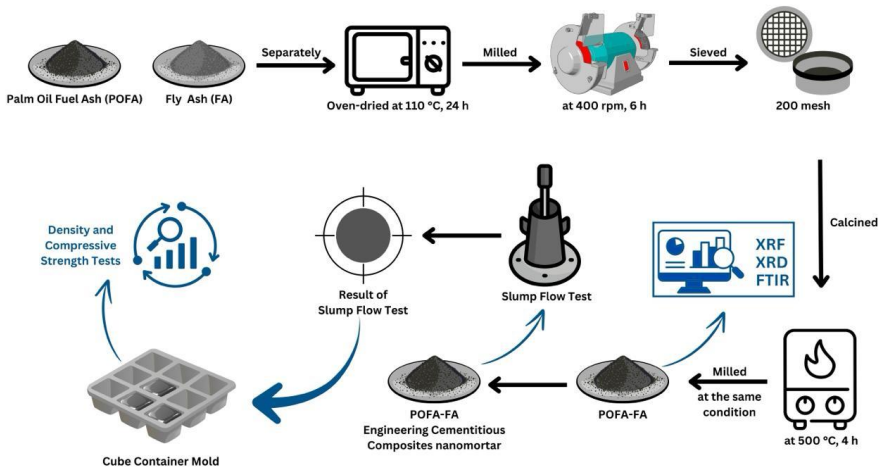

* Corresponding author: Siregar, Shinta Marito
✉ E-mail: shintamarito@umnaw.ac.id

Introduction

In Indonesia, the primary fuels used in industrial boilers and power plants are coal and palm kernel shells. The combustion of these fuels generates large quantities of fly ash (FA) and palm oil fuel ash (POFA) as waste by-products. POFA typically contains a high percentage of silica oxide (SiO_2), ranging from 48.5% to 61% [1–5].

Similarly, FA is recognized as a pozzolanic material [6–8], containing significant amounts of silica (SiO_2), alumina (Al_2O_3), iron oxide (Fe_2O_3), and calcium oxide (CaO), along with smaller quantities of potassium, sodium, titanium, and sulfur [9–13].

These chemical compositions indicate that both POFA and FA possess strong cementitious potential, allowing them to react effectively within the cement matrix of Engineering Cementitious Composites (ECC), thereby producing high-performance concrete. ECC, also known as Strain Hardening Cement-Based Composites (SHCC) or more popularly as "bendable concrete" [14], is a type of fiber-reinforced material designed to overcome the brittleness of normal concrete. ECC exhibits a strain capacity of about 3–7%, approximately 300 times greater than that of conventional concrete, which is only around 0.01% [15,16].

This superior ductility results from its micromechanically engineered matrix and the inclusion of reinforcing fibers such as polyvinyl alcohol (PVA) or high-density polyethylene (HDPE). Previous studies on ECCs and strain-hardening cementitious composites (SHCCs) have demonstrated continuous advancements in micromechanical design, fiber optimization, and matrix innovation to enhance ductility, crack control, and environmental performance. Initially developed as fiber-reinforced composites exhibiting strain hardening and multiple microcracking at low fiber volumes [17–19], ECCs have evolved through the incorporation of synthetic fibers such as PVA and HDPE, and hybrid systems using steel and polyethylene fibers to improve strength and energy absorption [19–21].

Concurrently, the cementitious matrix has transitioned from ordinary portland cement-based systems toward sustainable blends containing supplementary cementitious materials like FA, blast furnace slag, and limestone powder to improve durability, workability, and strain capacity [22–24].

These innovations have broadened ECC applications in structural and seismic resilience contexts, where their pseudo-ductile and self-healing behaviors enhance crack control and energy dissipation [25–27].

More recent trends emphasize eco-efficient ECCs utilizing industrial by-products to reduce carbon footprints while maintaining superior mechanical and durability performance [28,29].

Although extensive research on ECCs and SHCCs has explored fiber optimization, micromechanical design, and matrix enhancement to improve ductility and crack control, most studies have relied heavily on conventional cementitious materials such as Portland cement and FA. While these approaches have successfully advanced ECC performance, limited attention has been given to integrating alternative industrial by-products with high silica content, particularly POFA, despite its abundance and potential as a sustainable cementitious material. Furthermore, few studies have investigated the nanoparticle-scale modification of such by-products to enhance their pozzolanic reactivity and influence on ECC microstructure and mechanical properties. Therefore, this study aims to utilize POFA and FA as nanoparticle-based partial cement replacements to develop sustainable nanostructured ECCs with optimized cementitious reactions, improved compressive strength, and enhanced eco-efficiency. This approach not only contributes to high-performance concrete development, but also promotes value-added recycling, reduces air

pollution, conserves natural resources, and increases the economic value of industrial waste.

Materials and Methods

Materials

The POFA used in this study was obtained from the Tinjowan Palm Oil Plantation, located in Tinjowan Village, Simalungun Regency, Indonesia, while the FA was sourced from PT Socimas, Medan, North Sumatra, Indonesia. The other materials used in this study included Ordinary Portland Cement (OPC) as the primary binder, silica sand as fine aggregate, PVA fibres as reinforcement, water, and a high-range water-reducing admixture (superplasticizer) to improve workability.

ECC nanomortar manufacturing

The initial stage of this study involved the preparation of materials, where POFA and FA were processed into nanoparticles using a ball mill. Before milling, both POFA and FA were oven-dried at 110 °C for 24 hours to remove moisture. The dried materials were then ground using a ball mill at 400 rpm for 6 hours, sieved through a 200-mesh sieve, and subsequently calcined at 500 °C for 4 hours. The calcined powders were then milled again for another 6 hours at 400 rpm to obtain uniform nanoparticle POFA and FA. The nanoparticle POFA and FA were characterized using X-ray fluorescence (XRF) to determine their oxide composition, X-ray diffraction (XRD) to analyze crystal structure and size, and Fourier transform infrared spectroscopy (FTIR) to identify functional groups. The nanomortar ECC mixtures were prepared using OPC as the main binder, silica sand as fine aggregate, PVA fibers as reinforcement, water, and a superplasticizer to enhance workability. The POFA and FA were used as partial cement replacements in varying proportions. Each material (POFA and FA) was varied at 0%, 5%, 10%, and 15% by weight of cement, resulting in a total of 16 mix combinations, as shown in Table 1.

Table 1. Matrix of POFA and FA percentage variations in ECC nanomortar mixtures

Composition	POFA			
FA	0%	5%	10%	15%
0%	S1	S5	S9	S13
5%	S2	S6	S10	S14
10%	S3	S7	S11	S15
15%	S4	S8	S12	S16

Slump flow test

The slump flow test, a standard procedure to evaluate the flowability and workability of self-compacting or highly flowable concrete, was performed during the preparation of the POFA–FA ECC nanomortar. All constituent materials were prepared and weighed according to the designated mix proportions, and then mixed in a bucket using a drill mixer while recording the mixing time with a stopwatch. The total mixing duration was limited to 12 minutes to ensure uniform consistency. Before testing, all equipment was cleaned and dried. The Abrams cone was placed vertically on the base plate and held firmly to prevent movement. The POFA–FA ECC nanomortar mixture was then poured into the cone without tamping within 30 seconds. The cone was lifted vertically in one smooth motion to a height of approximately 30 cm, allowing the mixture to flow freely. The time required for the spread to reach a diameter of 500 mm (T_{500}) was recorded using a stopwatch immediately after lifting. The maximum spread diameter was then measured in two perpendicular directions (D_1 and D_2), and their average was taken as the slump flow value [30]. After the test, the mixture was poured into pre-oiled cube molds (15 cm × 15 cm × 15 cm) and cured for 3, 7, and 28 days, as shown in Figure 1. Density and compressive strength were subsequently measured at each curing age.

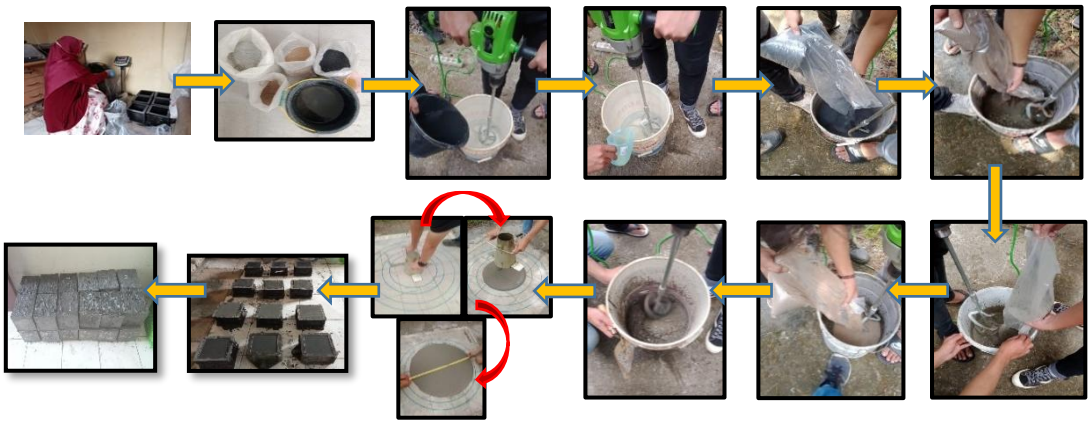

Figure 1. The manufacturing process of POFA–FA ECC nanomortar

Density and compressive strength tests

Density is defined as the mass of a sample per unit volume. According to Ahmad Zawawi *et al.* [4], the recommended density range for oil palm shell lightweight aggregate concrete incorporating FA is between 1.60 and 2.50 g/cm^3. The density test was carried out at the curing ages of 3, 7, and 28 days by measuring the mass and volume of each specimen. Before measurement, the specimens were surface-dried to remove excess moisture. The mass was determined using a digital balance, while the volume was calculated based on the specimen's dimensions. To determine the compressive strength of the ECC nanomortar, tests were conducted in accordance with SNI 1974:2011 using a Universal Testing Machine (UTM). The cube specimens (15 cm × 15 cm × 15 cm) were positioned centrally between the machine platens, and load was applied gradually at a uniform rate until failure occurred. The maximum load sustained by the specimen was recorded and used to calculate the compressive strength.

Results and Discussion

XRF analysis

Based on the results of the XRF test, the elemental and compound compositions of POFA and FA were determined. The chemical compositions obtained from the XRF analysis are presented in Table 2. For POFA, the dominant oxides identified were SiO_2 = 48.9%, Fe_2O_3 = 3.42%, and CaO = 13.8%. These values indicate that POFA possesses cementitious properties, as materials with a combined oxide content of SiO_2 + Al_2O_3 + Fe_2O_3 > 50% and CaO > 10% are classified as cementitious materials [31,32].

Table 2. Chemical composition of POFA and FA based on XRF analysis

Oxide compound	POFA (%)	FA (%)
Al_2O_3	-	14.0
SiO_2	48.9	29.3
P_2O_5	6.97	-
SO_3	4.10	-
K_2O	20.5	1.14
CaO_2	13.8	18.3
TiO_2	0.15	1.54
V_2O_5	-	0.05
Cr_2O_3	-	0.07
MnO	0.61	0.65
Fe_2O_3	3.42	30.9
NiO	-	0.03
CuO	0.15	0.06
ZnO	0.06	0.02
SrO	0.12	0.48
MoO_3	0.50	2.10
BaO	0.10	0.38
Eu_2O_3	0.10	0.38
Yb_2O_3	-	0.03
Re_2O_7	0.07	0.31

For FA, the chemical composition was SiO_2 = 29.3%, Al_2O_3 = 14%, Fe_2O_3 = 30.9%, and CaO = 18.3%. These values demonstrate that FA exhibits both cementitious and pozzolanic characteristics. According to established criteria, materials containing SiO_2 + Al_2O_3 + Fe_2O_3 > 50% and CaO > 10% are cementitious, while those with SiO_2 + Al_2O_3 + Fe_2O_3 > 70% are classified as pozzolanic [12,32,33].

The high silica (SiO_2) and alumina (Al_2O_3) contents in both POFA and FA indicate strong potential for these materials to act as supplementary cementitious materials (SCMs) in ECC formulations, enhancing pozzolanic reactivity and contributing to improved mechanical and durability performance.

XRD analysis

The XRD analysis results confirmed that POFA and FA particles were successfully synthesized using the top-down method via ball milling, with average crystal sizes of 28.02 nm for POFA and 16.47 nm for FA (Table 3). Phase identification was conducted using the Match! – Phase Identification from Powder Diffraction Data software and the Crystallography Open Database (COD). The identified crystalline phases of POFA and FA are presented in Figure 2 and Table 3.

As shown in Table 3, POFA contains two main crystalline phases: SiO_2 and $Ca_3(Si_3O_9)$. The SiO_2 phase exhibits a hexagonal crystal system with unit cell parameters a = 4.92 Å, b = 4.92 Å, and c = 5.42 Å, showing diffraction peaks at 2θ = 20.72°, 26.52°, 50.07°, 59.87°, and 68.04°, consistent with previously reported POFA nanoparticles [34].

The $Ca_3(Si_3O_9)$ phase exhibits a monoclinic crystal system with unit cell parameters a = 15.33 Å, b = 7.28 Å, and c = 7.07 Å, showing peaks at 2θ = 27.50° and 29.65°. The crystallite sizes, calculated from the FWHM, indicate nanoscale dimensions, confirming the nanoparticle nature of POFA. Meanwhile, FA nanoparticles exhibit a hexagonal crystal system with dominant SiO_2 phase, characterized by diffraction peaks at 2θ = 21.37° and 27.17°, and crystallite sizes around 16–17 nm. These XRD results confirm that both POFA and FA are suitable as nanosized cementitious materials.

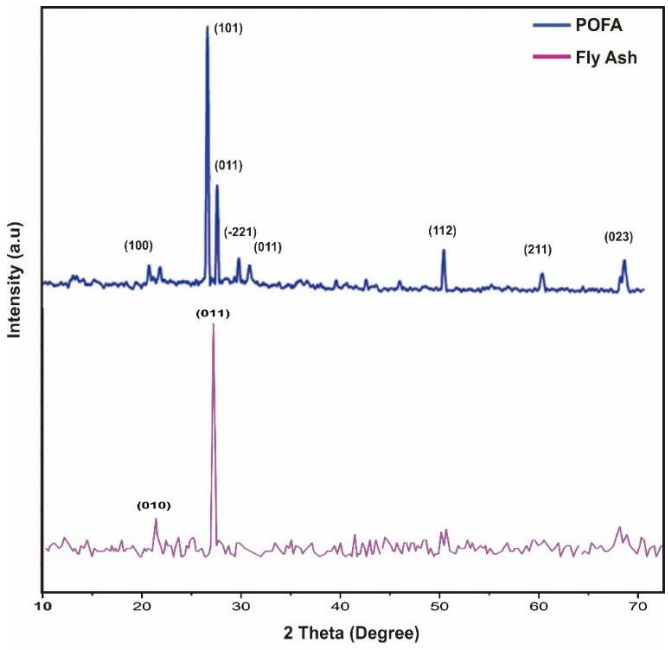

Figure 2. XRD patterns of POFA and FA samples

Table 3. XRD phase identification data of POFA and FA

Sample	No.	Peak position (2θ) (°)	FWHM (°)	Crystallite size (D) (nm)	Miller indices (hkl)	Interplanar spacing (d) (Å)
POFA	1	20.72	0.2255	35.82	100	4.27
	2	26.52	0.2288	35.67	101	3.36
	3	27.50	0.2105	38.85	011	3.25
	4	29.65	0.2286	35.94	-221	3.01
	5	30.73	0.3590	22.95	011	2.91
	6	50.07	0.2400	36.54	112	1.82
	7	59.87	0.3465	26.46	211	1.54
	8	68.04	0.4858	19.73	023	1.38
		Average		**28.02**		
FA	1	21.37	0.4819	16.78	010	4.15
	2	27.17	0.5061	16.15	011	3.28
		Average		**16.47**		

Note: *Shape factor (K) = 0.94; Wavelength (λ) = 1.5406 Å.*

The crystallinity of POFA and FA was also determined from the XRD analysis, as shown in Table 4.

Determining the proportion of amorphous and crystalline minerals in natural pozzolans is crucial for evaluating their oxide content. Previous studies have indicated that the amorphous phase represents the highly reactive alkali-active fraction. Although no general limit exists for the amorphous content in natural pozzolans, materials with less than 15% amorphous minerals have been shown to perform poorly as cement replacements [35].

Table 4 shows that POFA has a total area of 343.01 with a crystalline area of 96.81, corresponding to a crystallinity of approximately 28.22%, whereas FA has a total area of 500.83 with a crystalline area of 43.59, corresponding to a crystallinity of 8.70%. These values indicate that the amorphous fraction in both POFA and FA nanoparticles is significantly larger than the crystalline fraction. A higher proportion of amorphous content enhances compressive strength because the crystalline oxides in pozzolanic materials do not actively participate in pozzolanic reactions at room temperature. Pozzolanic activity occurs when the active silica and alumina in the pozzolan react with calcium hydroxide (CH) produced during cement hydration, forming irreversible molecular bonds known as calcium silicate hydrate (C–S–H) [36].

The C–S–H gel, often referred to as tobermorite, crystallizes and contributes to cement strength, while unreacted CH does not enhance strength and may weaken the cement over time. Typically, CH constitutes about 20% of the cement weight, and in the worst case, it can lead to structural separation due to CH leaching [37].

To mitigate this, additional silica-bearing pozzolanic materials such as POFA and FA are incorporated. In moist conditions, the pozzolan binds CH to form new C–S–H, enhancing concrete strength through the pozzolanic reaction [11,38].

FTIR analysis

The FTIR analysis was conducted to identify the functional groups present in POFA and FA. The results are presented in Figure 3. For POFA, characteristic peaks were observed at 797, 1,051, 1,362, 2,205, 2,266, and 3,615 cm^{-1}.

Table 4. Crystallinity of POFA and FA

Sample	Crystal area	Total crystal area	Total area	Crystallinity (%)
POFA	4.94	96.81	343.01	28.22
	7.82			
	41.76			
	16.22			
	6.16			
	6.62			
	8.56			
	4.75			
FA	12.34	43.59	500.83	8.70
	31.26			

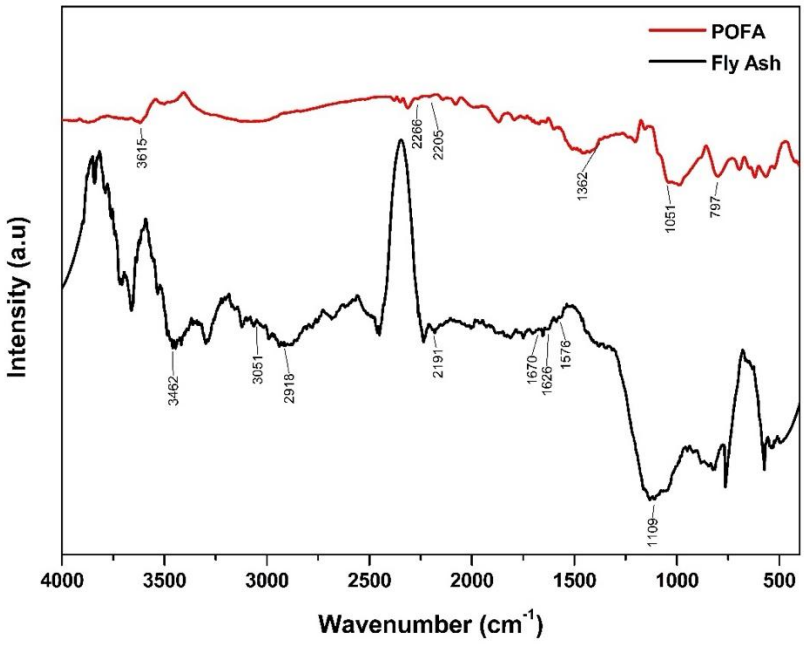

Figure 3. FTIR spectra of POFA and FA

The peak at 1,362 cm^{-1} corresponds to C–H bonds in alkanes with strong intensity. The peak at 797 cm^{-1} also indicates C–H bonds, this time in alkenes, with strong intensity. At 1,051 cm^{-1}, a C–O bond characteristic of alcohols was observed with strong intensity. The peak at 2,205 cm^{-1} corresponds to a triple bond C≡C in alkynes with variable intensity, while the peak at 2,266 cm^{-1} indicates a C≡N triple bond in nitriles with strong intensity. The peak at 3,615 cm^{-1} is associated with N–H bonds in amines with medium intensity. These results align with previous studies, where the O–H stretching vibration of SiOH groups absorbs in the region around 3,615 cm^{-1}, the asymmetric stretching vibration of Si–O is observed near 1,051 cm^{-1}, and the 797 cm^{-1} region corresponds to the crystalline quartz phase [39].

For FA, peaks were observed at 1,109, 1,576, 1,626, 1,670, 2,191, 2,918, 3,051, and 3,462 cm^{-1}. The peak at 1,109 cm^{-1} corresponds to C–O bonds in ethers with strong intensity. Peaks at 1,576 cm^{-1} and 1,626 cm^{-1} indicate C=C bonds in aromatic rings and alkenes, respectively, with variable intensity. The peak at 1,670 cm^{-1} corresponds to C=O bonds in aldehydes with strong intensity. The peak at 2,191 cm^{-1} indicates a C≡C triple bond in alkynes with variable intensity. Peaks at 2,918 cm^{-1} and 3,051 cm^{-1} correspond to C–H bonds in alkanes (strong) and alkenes (medium–strong), respectively. Finally, the peak at 3462 cm^{-1} corresponds to N–H bonds in amines with medium intensity. The O–H stretching vibration of SiOH groups absorbs near 3,462 cm^{-1}, while the Si–O–Si stretching vibration is observed around 1,109 cm^{-1} [39]. These FTIR results confirm the presence of key functional groups that contribute to the pozzolanic and cementitious activity of both POFA and FA in ECC nanomortar.

Slump flow test

The slump flow test was conducted to evaluate the workability of fresh ECC mortar, which reflects the ease of handling and placement of the mixture, expressed as a measurable value. Slump is defined as the vertical drop at the center of the concrete surface, measured immediately after removing the slump mold [40]. The slump value is influenced by the water-to-cement ratio (w/c), which is the weight ratio of water to Portland cement in the concrete mix. A higher w/c ratio results in a higher slump, producing a more fluid mixture that is easier to work with. However, increasing the w/c ratio also reduces compressive strength, so it should not exceed 0.5 [41]. In this study, a w/c ratio of 0.3 was used for all sample variations. This relatively low ratio is expected to enhance the compressive strength of the POFA–FA ECC nanomortar. To improve workability while maintaining the target w/c ratio, superplasticizer was added. The superplasticizer allows the mixture to flow more freely, filling the pores within the composite and reducing porosity, which in turn increases the density of the nanomortar. The slump flow results of the POFA–FA ECC nanomortar are shown in Figure 4. As observed, increasing the percentages of POFA and FA led to a decrease in slump flow values. This is due to the water-absorbing properties of POFA and FA particles, which reduce the mixture's workability. This observation aligns with previous studies reporting decreased workability in concrete mixes with FA, attributed to the water absorption characteristics of FA [41].

Despite this reduction, all compositions remained within the standard slump flow range for high-quality concrete (500–800 mm), indicating that all POFA–FA ECC nanomortar mixtures are still highly workable and easy to handle [42].

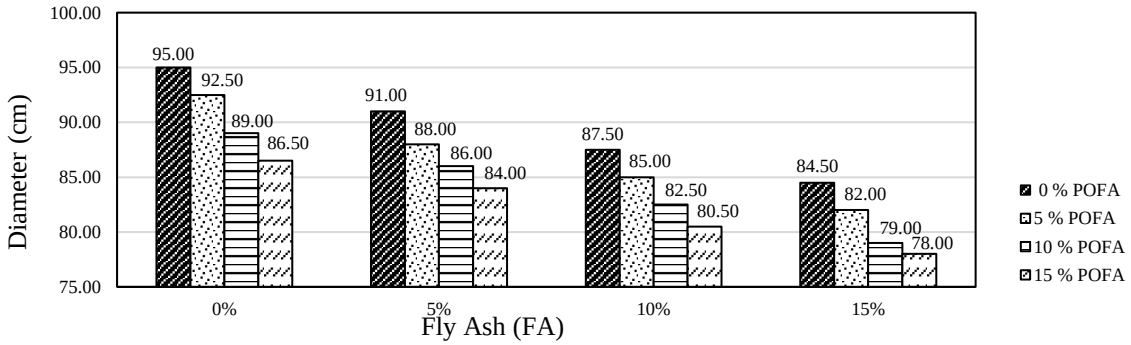

Figure 4. Slump flow test results of POFA–FA ECC nanomortar

Density test

Density is defined as the mass of a sample per unit volume and is also referred to as unit weight, specific gravity, or material compactness. The dry density of POFA–FA ECC nanomortar was measured to compare the effect of curing age at 3, 7, and 28 days. The results of the dry density tests are presented in Figure 5. As shown in Figure 5, the addition of POFA and FA reduces the density of the POFA–FA ECC nanomortar. Higher percentages of POFA and FA result in lower density, which can be attributed to the fine particle size of the nanoparticles affecting the compactness of the mixture. According to SNI 1973:2008 and ASTM C567, the density of normal concrete ranges from 2,200 to 2,400 kg/m^3. The densities observed in this study at 3, 7, and 28 days are lower than normal concrete but have not yet reached the typical range for lightweight concrete, which is 1,440–1,850 kg/m^3 [43,44].

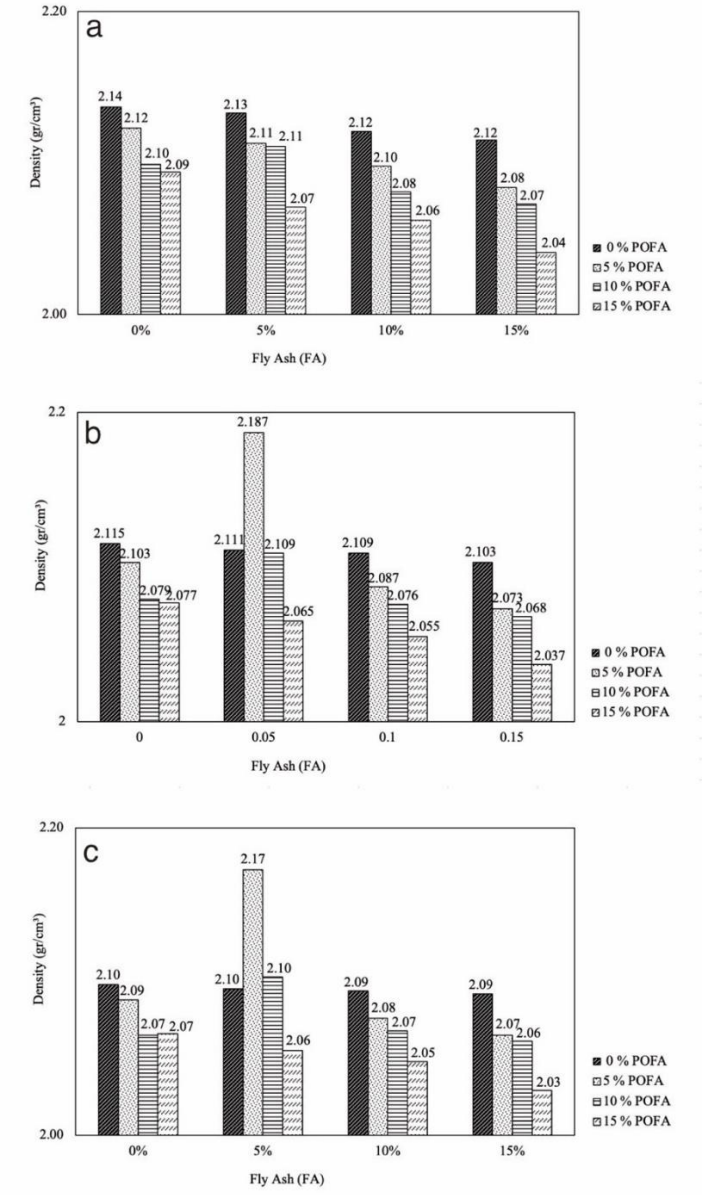

Figure 5. Dry density of POFA–FA ECC nanomortar at (a) 3 days, (b) 7 days, and (c) 28 days

Compressive strength

The compressive strength of POFA–FA ECC nanomortar was tested at 3, 7, and 28 days to evaluate the relationship between curing time and strength development. The results for 3 days, 7 days, and 28 days are presented in Figure 6.

At 3 days, the compressive strength ranged from 43.11 MPa to 58.09 MPa. After 7 days of curing, the strength increased to 45.21–65.78 MPa, and the maximum strength was observed at 28 days, reaching 46.34–72.73 MPa. This increase is attributed to the complete drying and hydration of the nanomortar at 28 days.

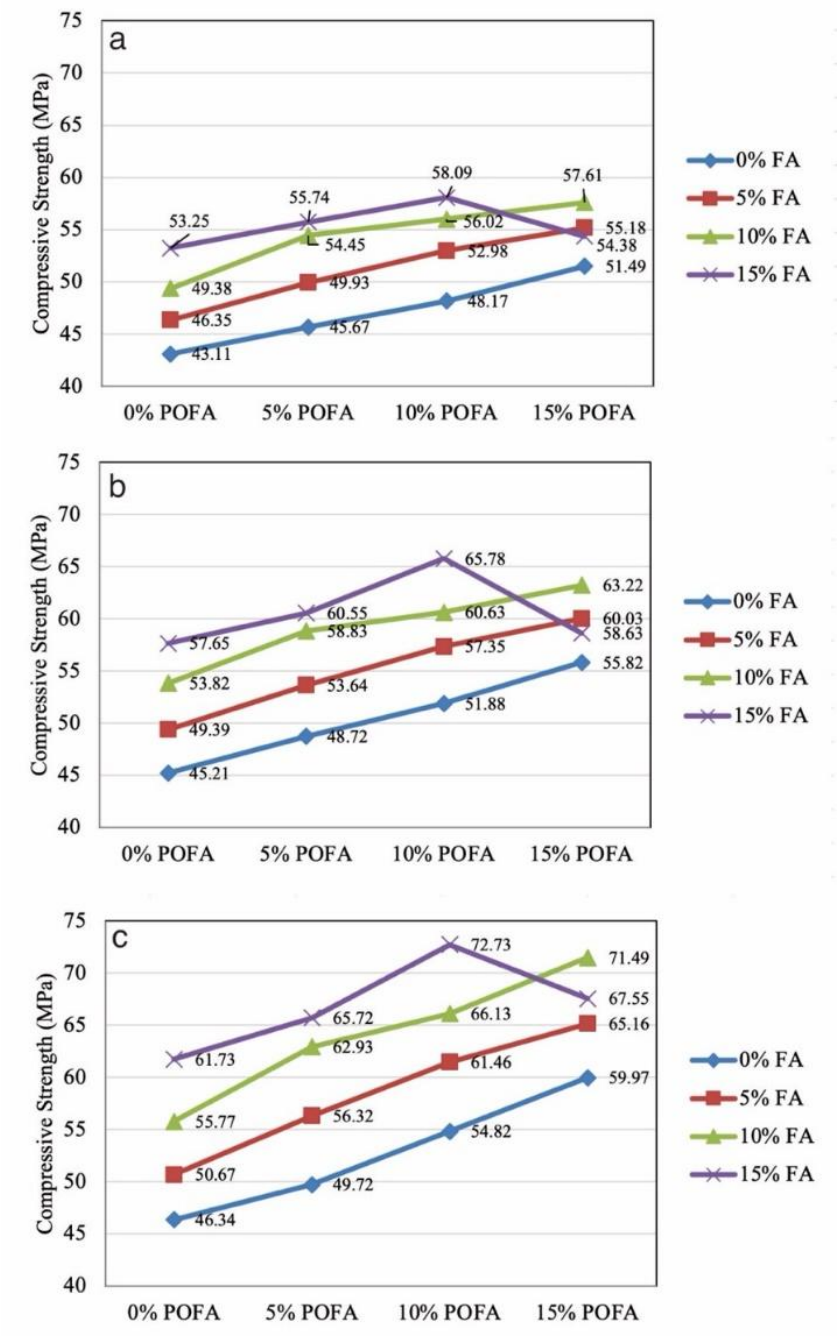

Figure 6. Compressive strength of POFA–FA ECC nanomortar at (a) 3, (b) 7, and (c) 28 days

Higher percentages of POFA and FA nanoparticles in the nanomortar corresponded to higher compressive strength. This indicates the contribution of SiO_2, Al_2O_3, Fe_2O_3, and CaO in POFA and FA as cementitious materials, which actively participate in the cement hydration process. According to SNI 03-1974:1990 and ASTM C 109, the compressive strength of normal concrete at 28 days ranges from 15 to 40 MPa [45]. The results confirm that all POFA–FA ECC variations exceeded the strength of normal concrete [46,47].

The highest compressive strength of 72.73 MPa was observed in the mix containing 10% POFA and 15% FA, using the same cement volume. Based on these results, all variations of POFA–FA ECC nanomortar qualify as high-strength concrete. High-strength concrete is defined as having a minimum compressive strength greater than 41.4 MPa [46] and is typically used in structural elements subjected to heavy loads, such as bridge girders, piers, pile foundations, sheet piles, and high-rise building structures. Using high-strength concrete allows for reduced structural dimensions, thereby lowering the overall weight of the structure. In practice, high-strength concrete often relies on finer and harder aggregates rather than large coarse aggregates to enhance strength and durability. In the production of high-strength concrete, the water-to-cement ratio (w/c) is carefully maintained between 0.2 and 0.3 to reduce porosity while preserving workability during placement, typically achieved through the addition of superplasticizers. Hydraulic cement hardens upon reacting with water. During this reaction, hydration occurs, releasing heat as the water–cement paste sets and binds the aggregate particles together. The incorporation of supplementary cementitious materials, such as POFA and FA, alongside Portland cement, enhances the workability of the concrete and reduces thermal cracking in massive structures by mitigating hydration heat. The silica (SiO_2) present in POFA and FA reacts with Ca $(OH)_2$ to form calcium silicate hydrate (C–S–H), the primary compound responsible for concrete strength. Ca $(OH)_2$, a product of cement hydration, is brittle and water-soluble; therefore, the presence of POFA and FA contributes to increased strength in POFA–FA ECC nanomortar.

Comparison with previous studies

As shown in Table 5, the POFA–FA composite achieved a maximum compressive strength of 72.7 MPa after 28 days, outperforming previously reported composites such as SPC15% + SS85% (60.5 MPa), HSSCC + SCM (50.4 MPa), and HSECC + DP 20% (44.1 MPa). This improvement is attributed to the enhanced pozzolanic activity of POFA and FA, which promotes additional formation of C–S–H gel and results in a denser microstructure.

Table 5. Comparison of compressive strength and density of POFA–FA nanomortar with previously reported cementitious composites

Composite	Age (days)	Compressive strength (MPa)	Density (g/cm^3)	Reference
Hollow glass microsphere	28	69.0	< 1.50	[48]
SPC15% + SS85%	28	60.5	Not reported	[49]
HSSCC + SCM	28	50.4	Not reported	[50]
HSECC + DP 20%	28	44.1	Not reported	[51]
POFA-FA ECC	28	72.7	1.45-1.85	This work

The density range of 1.45–1.85 g/cm^3 indicates that the POFA–FA composite can be classified as a lightweight, high-strength material, achieving an optimal balance between reduced unit weight and mechanical performance. These findings confirm

the effectiveness of the POFA–FA combination as a sustainable cementitious filler for producing high-strength, lightweight concrete materials.

Conclusion

This study successfully developed and characterized POFA–FA nanomortar (ECC) with varying proportions of POFA and FA. Material characterization using XRF, XRD, and FTIR confirmed that POFA and FA are cementitious and pozzolanic, with POFA exhibiting hexagonal SiO_2 and monoclinic $Ca_3(Si_3O_9)$ phases, while FA showed a dominant hexagonal SiO_2 phase. Both materials contained a significant amorphous fraction, enhancing their pozzolanic reactivity. Slump-flow tests indicated that all nanomortar mixtures maintained high workability within the standard range for self-compacting concrete (500–800 mm), although workability decreased slightly as the POFA and FA content increased due to water absorption by the nanoparticles. Dry density decreased with increasing nanoparticle content, ranging from 2.03 to 2.19 g/cm^3, classifying the mixtures as lightweight concrete. Compressive strength increased with higher POFA and FA content, reaching a maximum of 72.7 MPa at 28 days, surpassing conventional and previously reported composites. This improvement is attributed to the pozzolanic reaction of SiO_2, Al_2O_3, and CaO in POFA and FA, which promoted additional C–S–H gel formation, reduced porosity, and increased microstructural density.

Acknowledgments

The author would like to express sincere gratitude to the Directorate of Research and Community Service, Directorate General of Research and Development, Ministry of Higher Education, Science, and Technology of the Republic of Indonesia for the financial support provided through the 2025 Regular Fundamental Research Program, based on the Decree of the Director of Research and Community Service No. 0419/C3/DT.05.00/2025 dated May 22, 2025. This research funding was implemented under Master Contract No. 122/C3/DT.05.00 and Subcontract/Research Implementation Agreement No. 18/SPK/LL1/AL.04.03/PL/2025; 071/LPPI UMNAW/F.11/2-25.

Disclosure Statement

No potential conflict of interest was reported by the authors.

ORCID

Shinta Marito Siregar: 0000-0002-3464-8417
Fatimah Insani Harahap: 0009-0000-4359-5508
Ridwanto Ridwanto: 0000-0001-6851-6175
Khairiah Khairiah: 0009-0004-1024-3337

References

[1] Frida, E., Bukit, N., Bukit, F.R.A., Bukit, B.F. Effect of hybrid filler oil palm boiler ash–bentonite on thermal characteristics of natural rubber compounds. *Ecological Engineering & Environmental Technology*, **2023**, 24.

[2] Frida, E., Bukit, N., Sinuhaji, P., Bukit, F.R.A., Bukit, B.F. New material nanocomposite thermoplastic elastomer with low-cost hybrid filler oil palm boiler ash/carbon black. *Journal of Ecological Engineering*, **2023**, 24(2), 302-308.

[3] Bukit, B.F., Frida, E., Humaidi, S., Sinuhaji, P., Bukit, N. Optimization of palm oil boiler ash biomass waste as a source of silica with various preparation methods. *Journal of Ecological Engineering*, **2022**, 23(8).

[4] Zawawi, M.N.A.A., Muthusamy, K., Majeed, A.P.A., Musa, R.M., Budiea, A.M.A. Mechanical properties of oil palm waste lightweight aggregate concrete with fly ash as fine aggregate replacement. *Journal of Building Engineering*, **2020**, 27, 100924.

[5] Cahyo, N., Alif, H.H., Hapsari, T.W.D., Aprilana, A. Comparative boiler performance, fuel cost and emission characteristic of co-firing palm kernel shell with coal on circulating fluidized bed boiler: An experimental study. *2021 International*

Conference on Technology and Policy in Energy and Electric Power (ICT-PEP), **2021**, 17-21.

[6] John, S.K., Nadir, Y., Girija, K. Effect of source materials, additives on the mechanical properties and durability of fly ash and fly ash-slag geopolymer mortar: A review. *Construction and Building Materials*, **2021**, 280, 122443.

[7] Muthusamy, K., Jaafar, M.S., Azhar, N.W., Zamri, N., Samsuddin, N., Budiea, A.M.A., Jaafar, M.F.M. Properties of oil palm shell lightweight aggregate concrete containing fly ash as partial cement replacement. *IOP Conference Series: Materials Science and Engineering*, **2020**, 849(1), 012048.

[8] Xi, B., Zhou, Y., Yu, K., Hu, B., Huang, X., Sui, L., Xing, F. Use of nano-SiO_2 to develop a high performance green lightweight engineered cementitious composites containing fly ash cenospheres. *Journal of Cleaner Production*, **2020**, 262, 121274.

[9] Yu, J., Zhang, M., Li, G., Meng, J., Leung, C.K. Using nano-silica to improve mechanical and fracture properties of fiber-reinforced high-volume fly ash cement mortar. *Construction and Building Materials*, **2020**, 239, 117853.

[10] Zhang, P., Wang, K., Wang, J., Guo, J., Ling, Y. Macroscopic and microscopic analyses on mechanical performance of metakaolin/fly ash based geopolymer mortar. *Journal of Cleaner Production*, **2021**, 294, 126193.

[11] Alterary, S.S., Marei, N. Fly ash properties, characterization, and applications: A review. *Journal of King saud university Science*, 2021, 33, 101536.

[12] Amran, M., Fediuk, R., Murali, G., Avudaiappan, S., Ozbakkaloglu, T., Vatin, N., Karelina, M., Klyuev, S., Gholampour, A. Fly ash-based eco-efficient concretes: A comprehensive review of the short-term properties. *Materials*, **2021**, 14(15), 4264.

[13] Muthusamy, K., Budiea, A.M.A., Mohsin, S.M.S., Zam, N.S.M., Nadzri, N.E.A. Properties of fly ash cement brick containing palm oil clinker as fine aggregate replacement. *Materials Today: Proceedings*, **2021**, 46, 1652-1656.

[14] Ding, Y., Liu, J.P., Bai, Y.L. Linkage of multi-scale performances of nano-$CaCO_3$ modified ultra-high performance engineered cementitious composites (UHP-ECC). *Construction and Building Materials*, **2020**, 234, 117418.

[15] Zhang, Z., Liu, J.C., Xu, X., Yuan, L. Effect of sub-elevated temperature on mechanical properties of ECC with different fly ash contents. *Construction and Building Materials*, **2020**, 262, 120096.

[16] Zhou, Y., Zheng, S., Huang, X., Xi, B., Huang, Z., Guo, M. Performance enhancement of green high-ductility engineered cementitious composites by nano-silica incorporation. *Construction and Building Materials*, **2021**, 281, 122618.

[17] Li, V.C. On engineered cementitious composites (ECC) a review of the material and its applications. *Journal of Advanced Concrete Technology*, **2003**, 1(3), 215-230.

[18] Banaay, K.M.H., Cruz, O.G.D., Muhi, M.M. Engineered cementitious composites as a high-performance fiber reinforced material: A review. *GEOMATE Journal*, **2023**, 24(106), 101-110.

[19] Ahmed, S.F.U., Mihashi, H. A review on durability properties of strain hardening fibre reinforced cementitious composites (SHFRCC). *Cement and Concrete Composites*, **2007**, 29(5), 365-376.

[20] Yu, J., Li, V. Research on production, performance and fibre dispersion of pva engineering cementitious composites. *Materials Science and Technology*, **2009**, 25(5), 651-656.

[21] Kim, J.S., Cho, C.G., Moon, H.J., Kim, H., Lee, S.J., Kim, W.J. Experiments on tensile and shear characteristics of amorphous micro steel (ams) fibre-reinforced cementitious composites. *International Journal of Concrete Structures and Materials*, **2017**, 11(4), 647-655.

[22] Zhou, J., Qian, S., Sierra Beltran, M.G., Ye, G., van Breugel, K., Li, V.C. Development of engineered cementitious composites with limestone powder and blast furnace slag. *Materials and Structures*, **2010**, 43(6), 803-814.

[23] Figueiredo, S.C., Çopuroğlu, O., Šavija, B., Schlangen, E. Piezoresistive properties of cementitious composites reinforced by pva fibres. *International Conference on Strain-Hardening Cement-Based Composites*, **2017**, 709-717.

[24] Arivusudar, N., Babu, S.S. Mechanical properties of engineered cementitious composites developed with silica fume. *Cem. WapnoBeton25 (4)*, **2020**, 282-291.

[25] Xu, L., Pan, J., Leung, C.K.Y., Yin, W. Shaking table tests on precast reinforced concrete and engineered cementitious composite/reinforced

concrete composite frames. *Advances in Structural Engineering*, **2018**, 21(6), 824-837.
[26] Cho, C.G., Moon, H.J., Kim, H.Y., Lee, K.S. Seismic-improved reinforced-concrete composite column using a high-ductile fiber cementitious composite precast box. *Journal of Asian Architecture and Building Engineering*, **2019**, 18(2), 128-138.
[27] Dayyani, M., Mortezaei, A., Rouhanimanesh, M., Marnani, J.A. Performance of reinforced engineered cementitious composite square columns. *Građevinar*, **2023**, 75(1), 31-21.
[28] Hou, W., Lin, G., Li, X., Zheng, P., Guo, Z. Compressive behavior of steel spiral confined engineered cementitious composites in circular columns. *Advances in Structural Engineering*, **2020**, 23(14), 3075-3088.
[29] Zhang, H., Shao, Y., Zhang, N., Tawfek, A.M., Guan, Y., Sun, R., Tian, C., Šavija, B. Carbonation behavior of engineered cementitious composites under coupled sustained flexural load and accelerated carbonation. *Materials*, **2022**, 15(18), 6192.
[30] Amran, Y.M., Farzadnia, N., Ali, A.A. Properties and applications of foamed concrete; A review. *Construction and Building Materials*, **2015**, 101, 990-1005.
[31] Ginting, E.M., Bukit, N., Frida, E., Bukit, B.F. Microstructure and thermal properties of natural rubber compound with palm oil boilers ash for nanoparticle filler. *Case Studies in Thermal Engineering*, **2020**, 17, 100575.
[32] Siregar, S.M., Humaidi, S., Bukit, N., Frida, E. Analysis of coal boiler ash content and palm shell boiler ash as a cementitious material in ecc mortar. *Key Engineering Materials*, **2023**, 940, 165-172.
[33] Hamada, H., Alattar, A., Tayeh, B., Yahaya, F., Adesina, A. Sustainable application of coal bottom ash as fine aggregates in concrete: A comprehensive review. *Case Studies in Construction Materials*, **2022**, 16, e01109.
[34] Ginting, E.M., Wirjosentono, B., Bukit, N., Agusnar, H. Pengolahan abu boiler kelapa sawit menjadi nano partikel sebagai bahan pengisi termoplastik HDPE. *Majalah Polimer Indonesia,* **2015**, 18(1), 26–32.
[35] Reddy, P.N., Naqash, J.A. Experimental study on TGA, XRD and sem analysis of concrete with ultra-fine slag. *International Journal of Engineering, Transactions B: Applications*, **2019**, 32(5), 679-684.
[36] Nagrockienė, D., Girskas, G., Skripkiūnas, G., Daugėla, A. Properties of concrete modified by amorphous alumina silicate. *Engineering Structures and Technologies*, **2014**, 6(4), 178-183.
[37] Leemann, A., Shi, Z., Lindgård, J. Characterization of amorphous and crystalline ASR products formed in concrete aggregates. *Cement and Concrete Research*, **2020**, 137, 106190.
[38] Zhu, H., Zhang, D., Wang, T., McBain, M., Li, V.C. Intrinsic self-stressing and low carbon engineered cementitious composites (ECC) for improved sustainability. *Cement and Concrete Research*, **2021**, 149, 106580.
[39] Setiabudi, A., Hardian, R., Muzakir, A. Material characterization; principles and their applications in chemical research, Kedua ed., UPI Press: Bandung, **2016**.
[40] Standar Nasional Indonesia, *SNI 1972:2008 Cara Uji Slump Beton* **2008**.
[41] Akmal, A.M.N., Muthusamy, K., Yahaya, F.M., Hanafi, H.M., Azzimah, Z.N. Utilization of fly ash as partial sand replacement in oil palm shell lightweight aggregate concrete. *IOP Conference Series: Materials Science and Engineering*, **2017**, 271(1), 012003.
[42] ASTM, C. 1611/c 1611m: Standard test method for slump flow of self-consolidating concrete. *Annual Book of ASTM Standards*, **2009**, 4, 850-855.
[43] ASTM C567, Standard test method for determining density of structural lightweight concrete, **2009**.
[44] Standar Nasional Indonesia, *SNI 1973:2008 Cara Uji Berat Isi, Volume Produksi Campuran Dan Kadar Udara Beton* **2008**.
[45] Handayani, T. Memprediksi kuat lentur berdasarkan kuat tekan beton normal predicting flexural strength based on compression strength of normal concrete. *Jurnal Ilmiah Desain dan Konstruksi Vol*, **2019**, 18(2).
[46] SNI 03-1974, *Metode Pengujian Kuat Tekan Beton* **1990**.
[47] ASTM C109, *ASTM Int.* **2020**, *04*, 9.
[48] Lee, N., Pae, J., Kang, S.H., Kim, H., Moon, J. Development of high strength & lightweight cementitious composites using hollow glass microsphere in a low water-to-cement matrix. *Cement and Concrete Composites*, **2022**, 130, 104541.

[49] Prateek, G., Zheng, K., Gong, C., Wei, S., Zhou, X., Yuan, Q. Preparing high strength cementitious materials with high proportion of steel slag through reverse filling approach. *Construction and Building Materials*, **2023**, 368, 130474.

[50] Aditto, F.S., Sobuz, M.H.R., Saha, A., Jabin, J.A., Kabbo, M.K.I., Hasan, N.M.S., Islam, S. Fresh, mechanical and microstructural behaviour of high-strength self-compacting concrete using supplementary cementitious materials. *Case Studies in Construction Materials*, **2023**, 19, e02395.

[51] Zhang, M., Zhu, X., Pyo, S., Yang, Y., Liu, B., Shi, J. Feasibility of using high-volume pozzolanic fillers to develop sustainable engineered cementitious composites (ECC). *Powder Technology*, **2023**, 428, 118853.

HOW TO CITE THIS ARTICLE

S.M. Siregar, F.I. Harahap, R. Ridwanto, K. Khairiah. Synthesis and Characterization of Nano-Palm Oil Fuel Ash and Nano-Fly Ash as Cementitious Fillers in High-Performance Engineering Cementitious Composites. *Adv. J. Chem. A*, 2026, 9(6), 947-961.

DOI: 10.48309/AJCA.2026.554924.1955
URL: https://www.ajchem-a.com/article_238078.html